ELSEVIER

Pine sawdust modification using Fenton oxidation for enhanced production of high-yield lignin-containing microfibrillated cellulose

Ari Ämmälä [*,1], Juho Antti Sirviö [2], Henrikki Liimatainen [3]

Fibre and Particle Engineering Research Unit, University of Oulu, Oulu, Finland

ARTICLE INFO

ABSTRACT

Sawdust is an abundant high-quality residue from sawmills, representing 20–30 % of sawn products by volume. In this study, the chemical pre-treatment of pine sawdust with Fenton's reagent, formed from hydrogen peroxide and iron catalyst under moderately acidic conditions, was found to intensify the microfibrillation process in terms of energy consumption and improve the grade of the high-yield lignin-containing microfibrillated cellulose (LMFC) produced.

With a minor yield loss of 5.5 wt.%, Fenton pre-treatment increased the microfibrillation rate and bonding potential of LMFC, indicating that the ultrastructure of the lignocellulose cell walls had been modified. Linear dependency between the growth of specific surface area and energy consumption was seen, i.e. microfibrillation followed Rittinger's law of comminution. In comparison with the reference without any pretreatment, the total grinding energy consumption to a particle size of 14 μm was about 30 % lower (10.7 vs. 15 MWh/t) while the tensile strength and stiffness of LMFC films were 50 % (100 vs. 66 MPa) and 35 % higher (6.6 vs. 4.9 GPa), respectively. The advantageous effects of Fenton chemistry were assumed to originate from the cleavage of lignin-carbohydrate bonds, mainly between lignin and hemicelluloses. This phenomenon was supported by the substantially increased solubility of polysaccharides in dilute alkali.

The calculated manufacturing costs of LMFCs (using the above-mentioned specifications) was € 850/t, of which the raw material, chemical and electricity costs accounted for 10 %, 2 % and 88 %, respectively. Without any chemical pre-treatment, manufacturing costs were € 1100/t of which raw material accounted for 7 % and electricity 93 %.

1. Introduction

Sawn wood has an important role as long-term carbon storage (Packalen et al., 2017), and the goals of sustainable development promote its use as a renewable construction material. Globally, sawn wood originates mainly from coniferous species, at 74 % (FAO, 2020). It is noteworthy, however, that the sawmill industry produces a vast amount of waste wood, since only half of each log can be used for sawn products (Varis, 2018). The residuals, i.e. bark, sawdust and slab wood, account for 5–10 %, 10–15 % and around 30 %, respectively, of the total volume of incoming roundwood. Bark and sawdust are mainly used for energy production while chipped slab wood is usually used in pulp and paper production. The high moisture content of sawdust, which is about 50 %

for fresh wood, along with its low bulk density, means that it is not always logistically reasonable to use sawdust for energy production (i.e. heat, steam and electricity) unless energy can be produced on-site or near the site. This is often the case when a sawmill is situated in a rural area near raw material sources (forests), and the heating power of wood residuals would be surplus to local need. Additionally, energy production from wood waste has a low added value, and the full potential of wood components remains underutilized. Softwood sawdust is poorly suited for the production of high-quality pulp because the fibre length suffers considerably during sawing. However, sawdust is a clean, usually barkless, high-quality raw material, ideal for advanced uses such as lignin-containing microfibrillated cellulose, which could replace fossil-based raw materials in various applications, and thus lower the
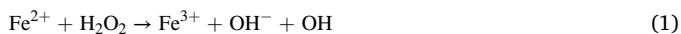
carbon footprint.

Compared to hardwood or non-woods, softwood has on average a higher lignin content and more recalcitrant nature, which is suggested to originate from its more branched lignin structure and more abundant carbon-carbon bonds (Liao et al., 2020). The potentiality of direct microfibrillation without the chemical pre-treatment of fast-growing hardwood has been demonstrated by Yousefi et al. (2018) while the microfibrillation of high-yield, non-delignified softwood pulp (i.e. mechanical pulp) has also been shown to be possible (Diop et al., 2017; Lahtinen et al., 2014; Osong et al., 2013; Serra-Parareda et al., 2021). Yet, the grade of lignin-containing microfibrillated cellulose (LMFC) or cellulose nanofibres (LCNF, also known as micro/nanofibrillated lignocellulose or wood nanocellulose) produced from softwood tends to remain poor and energy consumption high (Spence et al., 2011). One possibility to ease microfibrillation is the partial delignification of softwood, e.g. by alkali (Beluns et al., 2021a), sulphite (Hanhikoski et al., 2020) or the kraft method (Oliaei et al., 2021) at the expense of yield loss owing to the dissolution of lignin and hemicelluloses. However, there are ways to intensify microfibrillation by modifying the lignin-bearing cell wall without its delignification. Visanko et al. (2017) have shown that the grinding of softwood at or above the lignin-softening temperature is the key to the production of high-yield and high-grade microfibrillated cellulose having a lignin content close to the original softwood. More recently, the mild, neutral or alkaline sulphonation of lignin has been found to improve microfibrillation further because it reduces the lignin-softening temperature (Ämmälä et al., 2019) and enhances the bonding ability of LMFC by making lignin more hydrophilic (Ämmälä et al., 2021). LMFCs from non-delignified wood have been shown to serve as a reinforcement agent in papers and boards (Ämmälä et al., 2021; Serra-Parareda et al., 2021).

Moreover, the introduction of charged groups within the cell wall can facilitate the nanofibrillation of wood. Lignin-containing nanofibrils have been mechanically isolated through the TEMPO-mediated oxidation of hardwood (Herrera et al., 2018; Wen et al., 2019). Esterification has also been found to facilitate wood nanofibrillation (Iwamoto et al., 2019; Iwamoto and Endo, 2015). Lignocellulosic nanocrystals and nanofibrils have been produced mechanically from hardwood after maleic acid hydrolysis (Bian et al., 2017). Mechanochemical treatments in the presence of reactive deep eutectic solvents have recently been used for softwood without extensive yield losses. Fabrication of anionized (Sirviö and Visanko, 2017), cationized (Sirviö et al., 2020), sulphated (P. Li et al., 2019; Sirviö and Visanko, 2020) and succinylated (Sirviö et al., 2021) LCNFs from softwood has been demonstrated, making these functionalized LCNFs usable in applications like adsorption, non-flammable and antimicrobial barrier films, emulsion stabilization, reinforced green composites and UV shields.

The weakening of wood ultrastructure using Fenton chemistry could offer a novel approach for LMFC fabrication. Fenton's reagent, known since the 1890s, consists of a solution of H_2O_2 and an iron(II) salt such as $FeCl_2$ or $FeSO_4$. In acidic conditions, Fe(II) catalyses peroxide decomposition to create highly oxidative hydroxyl radicals ($OH^{\cdot}$), according to Eq. (1). The radicals formed are capable of oxidizing recalcitrant organic compounds by cleaving carbon-carbon double bonds and the benzene ring (Liu et al., 2017). For catalyst regeneration, ferric ion (Fe^{3+}) has to be reduced to ferrous form (Fe^{2+}), which can be done using either peroxide (Eq. (2)) or hydroxyl radicals (Eq. (3)) (Xie et al., 2015).

$$Fe^{2+} + H_2O_2 \rightarrow Fe^{3+} + OH^- + OH \quad (1)$$

$$Fe^{3+} + H_2O_2 \rightarrow Fe^{2+} + HO_2^{\bullet} + H^+ \quad (2)$$

$$Fe^{3+} + HO_2^{\bullet} \rightarrow Fe^{2+} + O_2 + H^+ \quad (3)$$

Fenton's reagent is widely used for treating wastewaters containing various organic pollutants, e.g. dyes, phenolic compounds and pharmaceutical substances (Wu et al., 2021) as well as for sewage sludges (Neyens and Baeyens, 2003). There are also several studies where

Fenton chemistry is used for the processing of lignocellulosic materials. In thermomechanical pulping (TMP), an interstage treatment between primary and secondary refiners with Fenton's reagent has been found to decrease the refining energy consumption by up to 35 % (Walter, 2013). Fenton chemistry has also been studied as a pre-treatment method to enhance the production of microfibrillated cellulose (Hellström et al., 2014) and cellulose nanofibrils (Duan et al., 2020; Q. Li et al., 2019) from bleached kraft pulp, i.e. with delignified pulp. In addition, numerous publications can be found related to the pre-treatment of biomass with Fenton's reagent prior to enzymatic hydrolysis and fermentation in the production of bioethanol (e.g. Yu et al., 2018) and biogas (Michalska et al., 2012).

The exact role of Fenton chemistry in the structural modification of lignocelluloses is not fully understood yet. It has been suggested that the non-enzymatic degradation of wood components, polysaccharides and lignin takes place via Fenton-based reactions, supposedly based on oxidative scissoring of polysaccharide chains and modifying the lignin by hydroxyl radicals (Arantes et al., 2011), resulting in the structural weakening of the microstructure of the fibre cell wall. Recently, Fenton chemistry has been reported to erode the lignin-hemicellulose layer surrounding the elementary fibril aggregates, thus loosening the structure of the aggregates by increasing the spacing between them (Zhu et al., 2020). This finding indicates that Fenton chemistry could also facilitate the microfibrillation of wood but, to the best of our knowledge, it has not been studied earlier for this application. Since the lignin moieties in the layer surrounding the fibril aggregates are covalently bound to carbohydrates, mainly to hemicelluloses (Zhao et al., 2020), it is postulated that the cleavage of those bonds by hydroxyl radicals, results in easier fragmentation of non-delignified wood matrix by mechanical forces in microfibrillation without causing a substantial yield loss.

In this paper we reveal how Fenton pre-treatment can intensify the direct microfibrillation of softwood sawdust (without any separate delignification step) in terms of energy consumption and the grade of LMFC. Especially, the particle size, nanofibril content, viscosity and the mechanical properties of films made from LMFC were studied. Moreover, a preliminary calculation of production costs of Fenton treatment for LMFC production using untreated and sulphite-pre-treated pine sawdust is presented.

2. Materials and methods

Air-dry pine (*Pinus sylvestris*) sawdust with a moisture content of 8 % was provided by Keitele Group (a sawmill in Central Finland). The particle size distribution measured by sieving is attached in the Supplementary material. The chemical composition of sawdust is presented in Table 2 (Pine ref). A solution of hydrated iron sulphate ($FeSO_4*7H_2O$) and hydrogen peroxide at a concentration of 30 wt.% was used as Fenton's reagent. H_2SO_4 and NaOH were used for pH adjustment of the solution.

2.1. Fenton treatment

Sawdust (300 g) having a median particle size of 0.7 mm was mixed with hot deionized water at a mass ratio of 1:9. Then, the pH of the dispersion was adjusted to 3.5 with H_2SO_4 and iron sulphate was added with the amount corresponding to 10–30 mg/L of Fe(II), and the mixture was mixed for five minutes. After that, peroxide was added (a concentration of 1.25–5.00 g/L, corresponding to 1.13–4.50 % of dry wood) and the mixture was allowed to react at a temperature of 75 °C in an oil bath for 45 min. Finally, the batch was dewatered on a wire sieve and washed four times with 2.5 dm^3 of deionized water in repeated dilution-dewatering cycles. The temperature and pH were recorded during the reaction.

The residual peroxide of the reaction solution was determined by iodometric titration of 25 mL of reaction solution with 0.01 M sodium

thiosulphate (Brandhuber and Korshin, 2009). The other reagents used were 10 mL of potassium iodine solution, 2 mL of sulphuric acid (2 M), three drops of ammonium molybdate solution and a few drops of starch solution as a colour change indicator.

The total organic carbon (TOC) of the filtrated reaction solution was measured with a Sievers 900 Portable Total Organic Carbon Analyser (GE Analytical Instruments, Boulder, CO, USA). TOC measurements were used to calculate yield loss (*YL*) caused by Fenton treatment. By assuming dissolved substances being mostly carbohydrates, the yield loss is calculated as follows:

$$YL = \frac{TOC}{0.45} \frac{x}{m} \frac{V}{} 100\% \tag{4}$$

where *TOC* is the total organic content is in the solution, g/L.

V is the volume of the solution, L.

m is the weight of sawdust in batch, g.

The value of 0.45 is the relative carbon content in carbohydrates (cellulose and hemicellulose).

2.2. Extruder pre-grinding

Before grinding, all samples were centrifuged within a wire bag to a moisture content of around 45 wt.%. Then, moist Fenton-modified sawdust was fed into a twin-screw extruder (Coperion ZSK 18 MEGA-lab, Germany). The temperature was set at 85 °C and the rotation frequency of the screws at 120 min⁻¹. The total (with no-load power) and effective (without no-load power) specific energy consumption (SEC_gross and SEC_net, respectively) was calculated based on the measured torque of the screws, grinding time and the dry mass of the sawdust batch (Ämmälä et al., 2021).

2.3. Microfibrillation

An MKCA6–2 J friction grinder (Masuko Sangyo Co., Ltd., Japan) was used for microfibrillation using a rotation frequency of 25 s⁻¹. A batch of pre-ground sawdust from the extrusion (100 g as dry mass) was diluted to a consistency of 1.7 wt.% with hot deionized water. The suspension was circulated from a vessel submerged in a hot water bath via the grinder with a peristaltic tube pump (Watson-Marlow Fluid Technology Group, USA). The grinding temperature was around 80 °C and the pH in the range of 5.5–6.0.

The rotor and stator clearance was initially adjusted to zero (contact mode). During the first 10 min of grinding, the gap was gradually reduced from zero to −90 μm and then grinding was continued for 50 min. After that, the gap was adjusted to −100 μm for the final 60 min of grinding. A small sample was taken for analyses every 30 min. Due to evaporation, the average grinding consistency was slightly higher than the initial consistency, at around 2.0–2.2 wt.%.

The total (with no-load power) energy consumption was recorded with an iEM3250 Schneider-Electric (Germany) energy meter. The effective energy consumption was calculated by subtracting the no-load power of the empty grinder using a positive clearance between the discs.

2.4. Characterization of pre-ground and microfibrillated sawdust from Fenton treatment

The chemical composition was measured from the samples after extrusion with the following methods: extractives in accordance with TAPPI T280, lignin in accordance with TAPPI T222, alkali-soluble polysaccharides in accordance with TAPPI T212, and ash in accordance with ISO 1762.

The volume-weighted particle size was measured with a laser diffraction analyser (Beckman Coulter LS 13 320, USA). Before the measurement samples were diluted to a consistency of 0.2 %, a dispersant was added (Sokolan CP5) and then the suspensions were mixed

with a magnetic stirrer for 25 min and in an ultrasonic bath for six minutes.

The analysis of the proportions of micro- and nanofibre fractions was conducted by centrifuging (Beckman Coulter Avanti J-26 XPI, USA) the LMFC suspension at a consistency of 0.2 % and a centrifugal force of 1252 G for 20 min (Serra-Parareda et al., 2021). The nanofibres were separated to the supernatant, while the microfibres settled in the sediment. The siphoned supernatant and sediment were dried at 105 °C, and the yield of nanofibres (*Y*) was calculated as follows:

$$Y = \frac{w_0}{w_{sed} + w_0} \tag{4}$$

where w_{sed} is the dry weight of the sediment, mg.

w_0 is the dry weight of the supernatant, mg.

The viscosity of the LMFC suspensions was measured at a temperature of 25 °C and at a consistency of 1 % with a DV-II + Pro EXTRA viscometer (Brookfield, USA). A vane-shaped spindle (V-73) and four rotational speeds (10, 20, 50 and 100 min⁻¹) were used.

The morphology of the micro- and nanofibre fractions was characterised using a field-emission scanning electron microscopy (FESEM) (JEOL JSM-7900F, Japan). Dilute sample dispersion was first filtrated on the membrane followed by freeze drying. A small piece of membrane was then attached to metal stub using carbon tape and sample was sputter-coated with platinum (high-resolution sputter coater, Agar Scientific, UK) using a sputtering time of 30 s and a current of 40 mA.

Chemical characterization of the sawdust/LMFC before and after Fenton treatment was performed using a Bruker Vertex 80 v (USA) diffuse reflectance infrared Fourier transform (DRIFT) spectrometer. Spectra were obtained in the 600–3800 cm⁻¹ range, and 40 scans were taken at a resolution of 2 cm⁻¹.

The crystalline structures were investigated using wide-angle X-ray diffraction (WAXD). Measurements were conducted on a Rigaku SmartLab 9 kW rotating anode diffractometer (Japan) using Co Kα radiation (40 kV, 135 mA) (λ = 1.79 030 nm). Samples were prepared by pressing tablets of dried samples (oven-dried for extruder ground samples and freeze-dried for MFC samples) to a thickness of 1 mm. Scans were taken over a 2θ (Bragg angle) range from 5° to 50° at a scanning speed of 10°/s, using a step of 0.5°. The crystallinity index (CrI) was calculated from the peak intensity of the main crystalline plane (200) diffraction (I_200) at 26.2° and from the peak intensity at 22.0° associated with the amorphous fraction of cellulose (I_am), according to Eq. (5):

$$CrI = \frac{I_{200} - I_{am}}{I_{200}} 100\% \tag{5}$$

Thermogravimetric (TGA) and differential scanning calorimetry (DSC) analyses were made simultaneously with a TA Instruments SDT 650 under nitrogen flow (150 mL min⁻¹). Each sample was heated from 40 °C to 900 °C at a heating rate of 2 °C min⁻¹.

2.5. Preparation of LMFC films and their testing

Self-standing films were made from the diluted LMFC suspensions at a consistency of 0.15 %. The suspensions were filtered on a polyvinylidene fluoride membrane (Durapore) having a pore size of 0.65 μm using a negative pressure of 70 kPa. The dewatered film was dried between two membranes in a Rapid-Köthen sheet dryer (Karl Schröder KG, Germany) under a vacuum of 0.15 bar at a temperature of 93 °C for 10 min (ISO 5269–2-:2004). Each film was conditioned at 23 °C in 50 % relative humidity (ISO 187) before measurements.

The film thickness was determined with a precision thickness gauge (Hanatek FT3, UK). Each film was weighed for density calculation and then cut into six 6-mm-wide strips for tensile strength measurement, which was performed using a Zwick D0724587 (Switzerland) material testing device with a 100 N load cell. The gauge length was 40 mm and the strain rate was 4 mm/min.

3. Results and discussion

3.1. Pre-tests with Fenton's reagent

3.1.1. Effects on TOC and peroxide consumption

In order to find suitable conditions for Fenton treatment, preliminary tests were done with various Fe(II) and H_2O_2 doses. The doses chosen were at a similar level to those used by Walter et al. (2009) in their study where TMP was treated with Fenton reagent after the primary refiner. The effects of the Fenton treatments were evaluated in terms of TOC and peroxide consumption in the reaction solution after 45 min of reaction (Table 1).

Sustaining an acidic pH – the optimal proposed value is 3–4 (Vasquez-Medrano et al., 2018) – during the reaction is essential in order to avoid the generation of Fe(III) ions, because ferrous iron may scavenge hydroxyl radicals causing precipitation of iron as $Fe(OH)_3$ at higher pH values (Tufail et al., 2020). In the pre-tests, the pH decreased slightly from the initial value of 3.5 to the end value of 3.1-3.3, except in the test where Fe(II) was not used (pH 3.6).

The consumption of peroxide indicates the potential amount of hydroxyl radicals formed during the reaction. It increased both with increasing Fe(II) and peroxide doses, but the peroxide dose had a lesser role than the Fe(II) dose. The increase in the peroxide dose from 1.25 to 5 g/L increased the peroxide consumption from 0.94 g/L to 1.24 g/L, while increasing the Fe(II) dose from 10 mg/L to 30 mg/L increased peroxide consumption from 0.66 g/L to 1.69 g/L. Interestingly, even without the addition of Fe(II), 0.81 g/L of peroxide was consumed, suggesting that the peroxide is consumed via oxidation reactions with the organic and inorganic components of wood.

The TOC increased with increasing Fe(II) content; at a constant H_2O_2 dose of 2.5 g/L, TOCs of 2530, 2810 and 2860 ppm were measured with Fe(II) doses of 10, 20 and 30 mg/L, respectively, while H_2O_2 doses of 1.25, 2.5 and 5 g/L TOCs of 2630, 2810 and 3130 ppm were recorded, respectively. Without Fe(II), the TOC was at quite a high level (1730 ppm), demonstrating the oxidation of sawdust by acidic peroxide which increased the hot-water-soluble substances, presumably originating mainly from hemicelluloses (Kishani et al., 2018). Although a trace of heavy metals in the wood might cause formation of radicals, the unchanged final pH did not indicate this.

The yield loss is directly related to dissolved organic substances; thus TOC can be used instead of the gravimetric determination of yield (Rööst and Jönsson, 2001). Fenton chemistry generates dissolved substances, which are mainly sugars and carboxylic acid (Jeong et al., 2021). Acidic peroxide without Fe(II) caused a loss of 3.4 %. With Fe(II) the loss increased and varied between 5.0 % and 6.1 %, which is in line the losses reported earlier (about 3 %) under similar reaction conditions but with half the reaction time (Walter et al., 2009).

3.1.2. Effects on extruder pre-grinding

Among the Fenton's reaction parameters tested, no significant differences were found in energy consumption or particle median size after pre-grinding (Table 1). Fenton treatment, however, increased the energy consumption during the extruder pre-grinding in comparison to the reference: the energy consumption was approx. 20 % higher. In pre-grinding, energy is consumed by fibre separation and especially fibre cutting. Fibre separation from the wood matrix occurs along the middle lamellae or randomly across the cell wall. It is possible that acidic conditions changed the topochemistry between the cell wall and the middle lamellae (Xu et al., 2020), thus having a detrimental effect on fibre separation.

Fenton treatment visibly lowered the brightness of wood, as can be seen in Fig. 1. This may originate from the coloured compounds formed by iron-lignin and iron-extractive complexes (Walter, 2013) or the formation of chromophores via lignin oxidation (Xie et al., 2015).

3.2. Microfibrillation

Fenton 3, which represents an "average" of the pre-tests, was chosen for more precise examination and further microfibrillation experiments. In that experiment, a clear effect measured as TOC was seen with moderate peroxide and iron salt doses. The effects of Fenton pre-treatment on microfibrillation were compared to the reference, which was treated identically (excluding chemical pre-treatment), from the same raw material. This data has been published earlier by Ämmälä et al. (2019).

3.2.1. Chemical composition

The chemical composition measured after extrusion pre-grinding is presented in Table 2. The results show that the use of Fenton chemistry for the pre-treatment of sawdust did not change the lignin content although it increased the solubility of polysaccharides into dilute alkali significantly, from 14.8 % to 25.3 %. The amount of dissolved carbohydrates aligns well with the hemicellulose content (26–27 %) of Scots pine reported by Kilpelainen et al. (2003) and Normark et al. (2014). This result implies that hydroxyl radicals cleave the bonds between lignin and carbohydrates, in particular those between the hemicelluloses. This is also supported by previous results indicating that Fenton chemistry can break bonds, mostly between xylan and lignin, and, to a lesser extent, bonds between lignin and glucan or glucomannan (Jeong et al., 2021).

Fenton chemistry was ineffective in decreasing the content of extractives, resulting in less than 20 % removal efficiency. This finding was expected as pine wood extractives consist mainly of resin and fatty acids that have a low solubility in acidic conditions.

The DRIFT and TGA results are attached in the Supplementary material. No significant changes between the IR spectra of the samples were found before and after Fenton treatment. Either the TGA and DSC analyses did not show any differences in thermal decomposition between the untreated and Fenton samples.

The XRD measurement results (see Supplementary material) show that the crystallinity index was slightly higher after Fenton treatment (58 % vs. 55 %) due to a minor dissolution of amorphous components, i. e. hemicelluloses and lignin. Masuko grinding decreased crystallinity as expected based on the results of Yousefi et al. (2018). After 120 min grinding, crystallinity index was 40 % for the untreated and 39 % for the pre-treated pine sawdust. A slightly higher drop in the crystallinity of the Fenton-treated sample is an indication of more absorbed energy during microfibrillation rather than the destruction of crystallinity by

Table 1

Effects of Fenton treatment processing conditions on final pH, residual peroxide, TOC, yield loss, energy consumption and median particle size after pre-grinding.

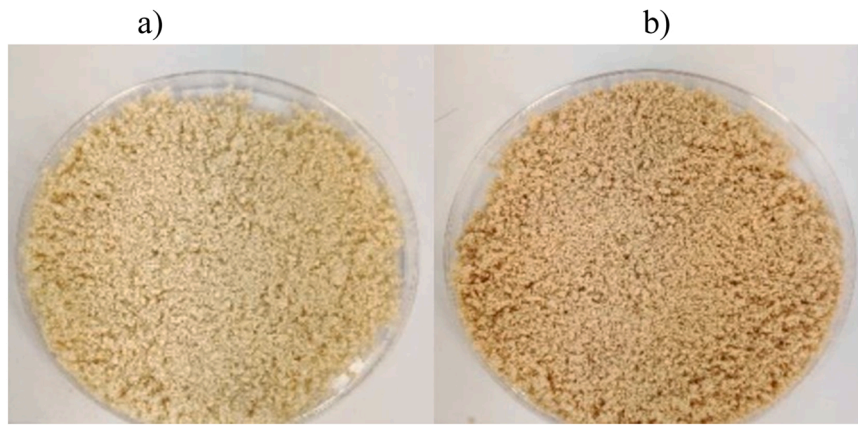| Entry	H_2O_2, g/L	Fe (II), mg/L	End pH	Consumed H_2O_2, g/L	TOC, ppm	SEC$_{gross}$, kWh/t	Particle size, µm	Yield loss, %
Fenton 1	2.5	0	3.59	0.81	1730	992	78.9	3.4
Fenton 2	2.5	10	3.34	0.66	2530	1006	67.6	5.0
Fenton 3	2.5	20	3.19	1.12	2810	1000	90.6	5.5
Fenton 4	2.5	30	3.05	1.69	2860	1000	89.6	5.6
Fenton 5	1.25	20	3.29	0.94	2630	1022	81.1	5.2
Fenton 6	5	20	3.15	1.26	3130	983	82.5	6.1
Pine ref*	–	–	–	–	–	830	79.0	–

*Data from Ämmälä et al. (2019).

Fig. 1. Pre-ground a) reference sawdust (on the left) and b) Fenton-treated sawdust (Fenton 3, on the right).

Table 2
Chemical composition of samples.

Sample	Extractives, %	Lignin, %	Alkali-soluble polysaccharides, %	Alkali-insoluble polysaccharides, %	Ash, %
Fenton	3.9	28.7	25.3	41.9	0.2
Pine ref. *	4.7	28.5	14.8	51.8	0.2

*Data from Ämmälä et al. (2019).

hydroxyl radicals.

3.2.2. Particle size and nanofibre content

The particle size distributions during the microfibrillation process are presented in Fig. 2. The decrease in median particle size from 79 μm to 15.7 μm for the reference and from 91 μm to 9.3 μm for Fenton pre-treated sawdust was achieved after 120 min of microfibrillation. SEM images of LMFC samples after microfibrillation are presented in the Supplementary material. The images show that the LMFCs are heterogeneous in nature. They also indicate that microfibrillation did not disintegrate the fibre cell wall to the elementary fibril level but that the sample consists of fibril aggregates having a width of tens of nanometres or fibril aggregate clusters and ribbons having a width of hundreds of nanometres.

Although a laser diffractometer has limitations in determining the dimensions of non-spherical particles with a high aspect ratio, the progress in size reduction is apparent. Additionally, the relationship between size reduction and energy consumption in the microfibrillation stage (pre-grinding excluded) followed the well-known Rittinger's law, which states that the size reduction energy per unit mass is directly proportional to the new specific surface area generated (Naimi et al., 2016). Since the specific surface area is inversely proportional to the particle size, the relationship can be presented as follows:

$$E = K \left(\frac{1}{x_p} - \frac{1}{x_f} \right) \tag{6}$$

where E is the specific energy, MWh/t.

x_p is the median size of the product, μm.

x_f is the median particle size of the feed, μm.

K is the parameter characterizing material properties.

As shown in Fig. 3, the slope (K in Eq. (6)) of the reference is 50 % steeper than in Fenton, i.e. 50 % more microfibrillation energy was required for equal growth of the specific surface area of particles. This phenomenon demonstrates that the Fenton pre-treatment favourably alters the material properties of pine sawdust. Weakening of the ultra-structure of wood matrix presumably took place via the cleavage of bonds between lignin and hemicelluloses due to attack by hydroxyl radicals, thus causing a decrease in the energy needed for the liberation of nano and microfibres by mechanical shear between the grinding discs.

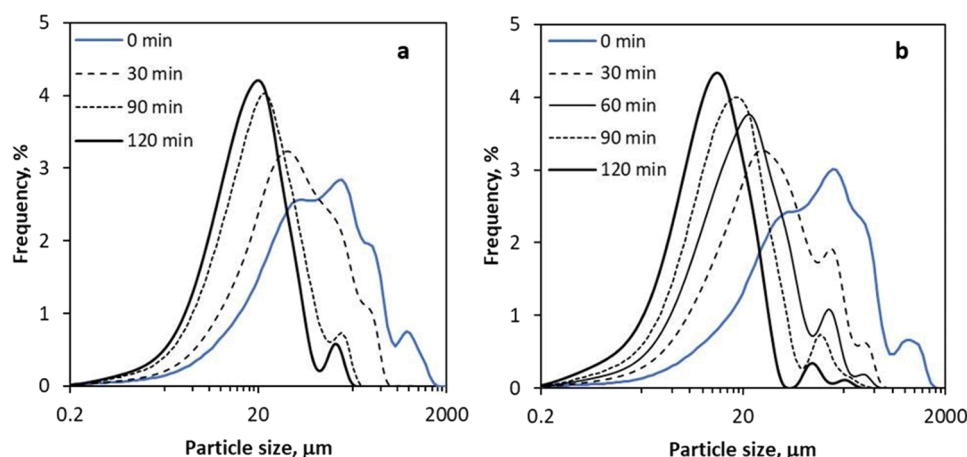The nanofibre content was determined by the centrifugation of

Fig. 2. Development of volumetric particle size distributions during microfibrillation: a) pine reference on the left, b) Fenton-treated on the right.
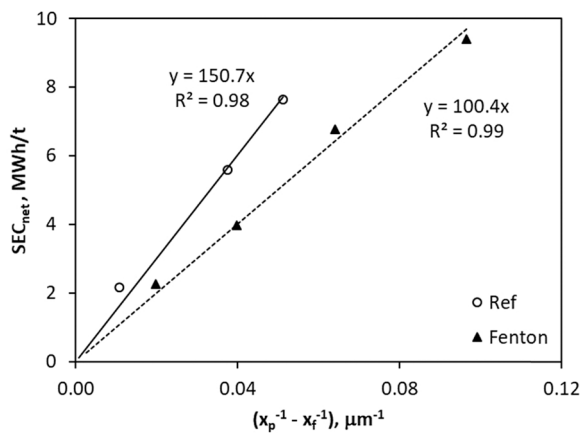
Fig. 3. Linear dependency on the specific energy consumption required for particle size reduction in the microfibrillation stage.

Fenton pre-treated sawdust after 0, 30, 60, 90 and 120 min of microfibrillation. As shown in Fig. 4, a large proportion (8 %) of the nanofibres was generated already in pre-grinding with the extruder. Extrusion grinding is a harsh method, causing severe fibre cutting and disintegration of the fibre cell wall, loosening its structure and liberating nanofibres.

During microfibrillation, the nanofibre yield increased fairly linearly with the energy applied. The yields also had a linear correlation to the inverse particle sizes, as was expected according to Eq. (5). The nanofibre yields were within the range of an LMFC made from bleached TMP pulp (Serra-Parareda et al., 2021), but in their study the grinding energy consumption was higher overall. This can be explained by the dissimilar microfibrillation set-ups; grinding is a more energy-efficient method than homogenization (Spence et al., 2011).

3.2.3. Viscosity

A low suspension viscosity is a characteristic feature of LMFC made from non-delignified wood (Ämmälä et al., 2021) and mechanical or chemi-mechanical pulp (Lahtinen et al., 2014; Visanko et al., 2017); Fenton pre-treatment resulted in similar rheological behaviour of the LMFC suspensions. As demonstrated earlier with an increase in the lignin content of LMFCs, the viscosity of the suspension decreases and the gel-like viscoelastic behaviour weakens (Yuan et al., 2021). It seems that the presence of lignin makes nano- and microfibres stiffer, less hygroscopic and less polar than microfibres based on bleached pulp.

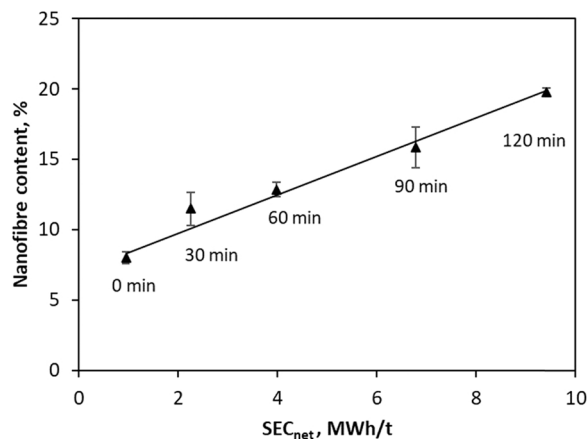The Fenton pre-treated LMFC (Fig. 5a) had a slightly higher viscosity

Fig. 4. Nanofibre content of LMFC made from Fenton pre-treated sawdust as a function of specific grinding energy consumption (microfibrillation times denoted).

than the reference LMFC (Fig. 5b); however, in general, viscosity was at a low level in comparison to any MFC made from bleached cellulose (Ämmälä et al., 2021), indicating that the micro- and nanofibrils of LMFC are in a less swollen state and are morphologically different from MFC. The viscosity of LMFC initially increased steeply with increasing microfibrillation energy but then started to decrease. This was evident both with the Fenton and the reference LMFCs, and occurred at all the tested rotational speeds although it was more prominent at lower shear rates. Similarly, shear-thinning behaviour became more pronounced with the increase in energy absorbed in microfibrillation but then started to diminish and almost disappeared at higher energy consumption, thus showing almost Newtonian, or probably more Bingham-like plastic behaviour as viscosity was independent of the shear rate. This was seen for Fenton pre-treated samples after 120 min of microfibrillation. For the reference, a longer grinding time would presumably have been needed.

The peculiar behaviour of LMFC viscosity can be explained as a number of micro- and nanofibre contacts that is proportional to the volume concentration and square of the aspect ratio, and as network forces that depend on the stiffness of the constituents and interfibrillar friction (Switzer and Klingenberg, 2004). At the beginning, the microfibrillation viscosity peaks because the aspect ratio increases rapidly as the number of large fibre bundles and aggregates disintegrate into stiff microfibres. Besides friction, there may also exist mechanical interlocking between rugged fibres. As the grinding continues, the stiffness of the microfibres starts to diminish due to a decrease in their width. At the same time, the friction and interlocking may also start to decrease due to the less rough surfaces of the microfibres. Finally, the viscosity starts to drop more rapidly as the grinding continues. The stiffness of the microfibres decreases further, as does the friction since the surfaces become smooth. The aspect ratio may start to decrease due to particle cutting. It is also possible that colloidal non-fibril-like lignin particles proliferate, disturbing fibre-to-fibre contacts, which in turn impairs network strength and reduces friction.

3.2.4. Mechanical properties

Self-standing films were fabricated from LMFCs with various microfibrillation times; the key results are listed in Table 3. Specific energy consumption is presented both with (SEC$_{gross}$) and without no-load power (SEC$_{net}$). The stress-strain behaviour of the films, as illustrated in Fig. 6, shows the typical characteristic shape of the elastic-plastic deformation of an MFC network: a linear elastic deformation without permanent failures followed by a plastic deformation and strain hardening until the failure of the films.

Consolidation of the films increased with increasing grinding time, as indicated by the increase in film density. Smaller particles with increasing specific surface area allowed denser packing and promoted bonding that facilitates interfibrillar stress transition during loading. Density has also been noticed to be a key indicator for the development of mechanical properties of (nano)fibre networks in previous studies (Amini et al., 2020; Niskanen, 1993). When comparing mechanical properties between the Fenton pre-treated and the reference samples by interpolating to a given particle size or density, it was observed that Fenton treatment resulted in an improved tensile strength and stiffness (see Fig. 7). Thus, the result demonstrates that Fenton pre-treatment has a positive effect on the chemical state of surfaces of LMFCs, promoting hydrogen bonding. This may be an indication of hemicelluloses playing an increasing role in bond formation.

In respect of mechanical properties, the microfibrillation rate for Fenton pre-treated sawdust was clearly faster than in the reference, i.e. development of tensile strength and stiffness was enhanced as a function of the microfibrillation energy applied. Strength development as a function of SEC was close to that of mildly sulphonated pine sawdust (Ämmälä et al., 2019) up to the maximum tensile strength of 100 MPa (82 kNm/kg) with a SEC$_{net}$ of 6.4 MWh/t. At higher SECs, tensile strength decreased considerably. If lower strength at break were related
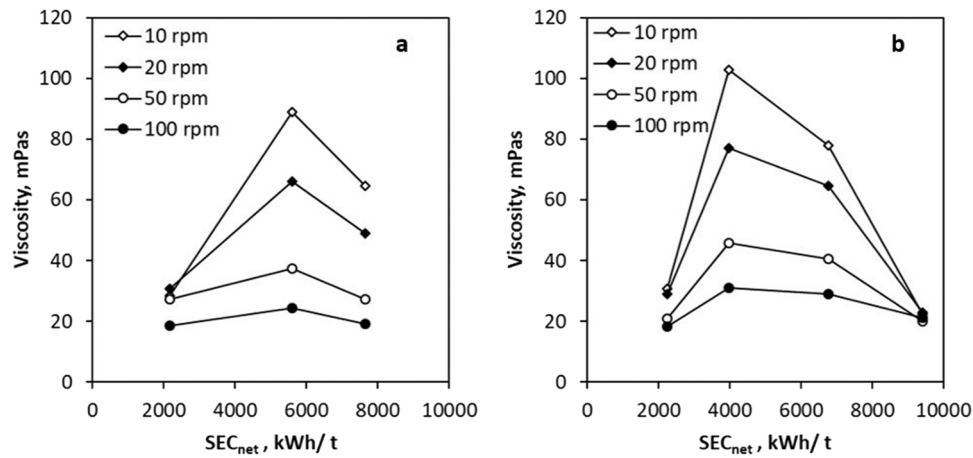
Fig. 5. Rotational viscosity of LMFC suspensions at a consistency of 1 % at various shear rates (i.e. rotational speeds of spindle); a) pine reference on the left and b) Fenton-treated on the right.

Table 3
Specific energy consumption with (SEC$_{gross}$) and without no-load power (SEC$_{net}$) and mechanical properties of self-standing films made from LMFC.

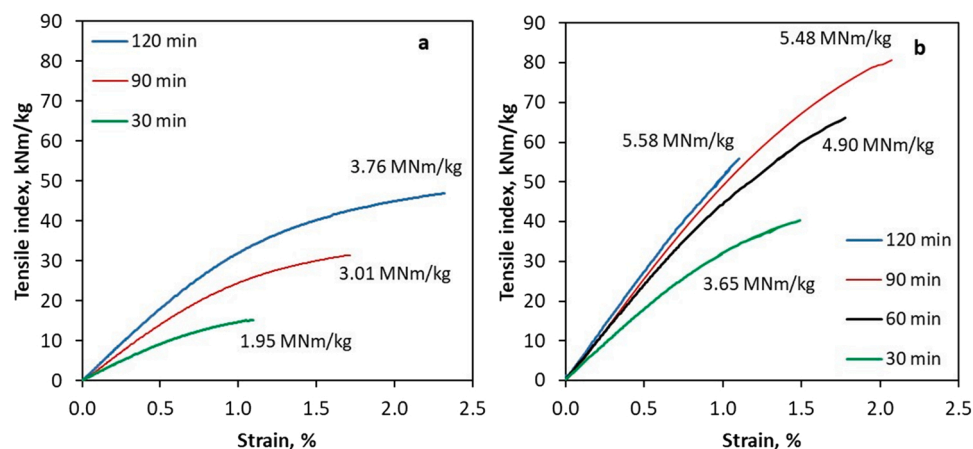| Entry	Pre-grinding & microfibrillation energy		Density	Tensile strength index	Tensile strength	Tensile stiffness index	Tensile stiffness	Strain	Median particle size
	SEC$_{gross}$ kWh/t	SEC$_{net}$ kWh/t	kg/m^3	kNm/kg	MPa	MNm/kg	GPa	%	μm
Ref 30 min*	3315	2153	676 ± 116	15.1 ± 1.3	10 ± 0.6	1.9 ± 0.2	1.3 ± 0.1	1.1 ± 0.1	42.6
Ref 90 min*	9568	5588	1143 ± 111	31.4 ± 2.9	36 ± 3.8	3.0 ± 0.2	3.4 ± 0.2	1.5 ± 0.5	19.9
Ref 120 min*	13 312	7645	1144 ± 54	45.3 ± 3.1	52 ± 4.1	3.8 ± 0.2	4.3 ± 0.2	2.4 ± 0.3	15.7
Fenton 30 min	3510	2252	557 ± 37	38.2 ± 1.0	21 ± 0.6	3.6 ± 0.1	2.0 ± 0.1	1.4 ± 0.1	32.6
Fenton 60 min	6550	3979	948 ± 47	65.8 ± 3.2	62 ± 3.1	4.9 ± 0.1	4.6 ± 0.1	1.8 ± 0.2	19.7
Fenton 90 min	10 798	6777	1220 ± 91	82.0 ± 4.2	100 ± 5.2	5.5 ± 0.2	6.7 ± 0.2	2.0 ± 0.2	13.3
Fenton 120 min	15 046	9407	1311 ± 46	54.6 ± 12.3	72 ± 16.1	5.6 ± 0.2	7.3 ± 0.3	1.1 ± 0.3	9.3

*Data from Ämmälä et al. (2019).

Fig. 6. Stress-strain behaviour of LMFC at various grinding times; a) pine reference on the left and b) Fenton-treated on the right. Respective tensile stiffness indexes are denoted beside the curves.

to a shorter fibre length and lower aspect ratio, then a decrease in stiffness should also be seen. However, the elastic modulus increased slightly, as shown in Fig. 6 (right). It is possible that the drop in tensile strength was due to the cumulative liberation of colloidal lignin and lignin nanoparticles during grinding. It has been suggested that lignin nanoparticles attach to the nanofibre surfaces and thus reduce hydrogen bond formation (Rojo et al., 2015). Due to the elevated temperature and vacuum used in the drying of the films, lignin might cement the
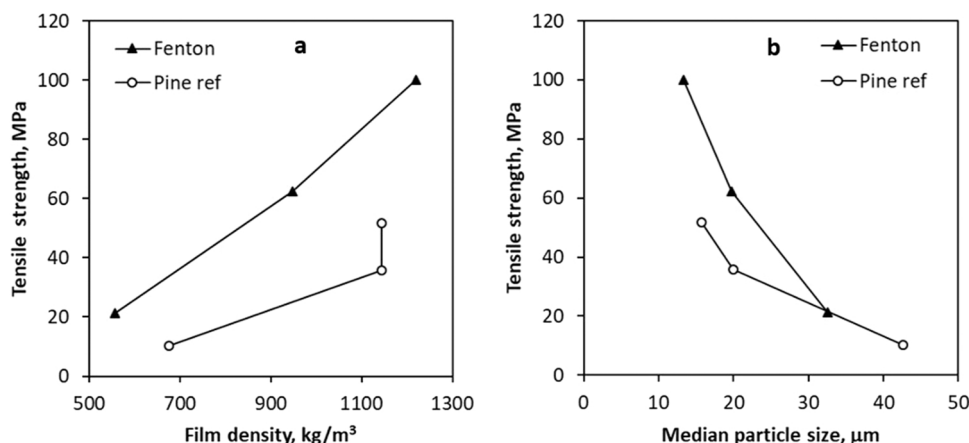
Fig. 7. Tensile stiffness as a function of density (a, on the left) and particle size (b, on the right).

nanofibre structure through crosslinking reactions between lignin and hemicelluloses (Oliaei et al., 2021) strongly enough that the film is broken without plastic elongation. In that case, the elastic modulus, i.e. tensile stiffness, is not affected because it is greatly dependent on density, which in a well-bonded network is directly related to the elastic modulus of fibres (Niskanen, 1993). Although the elastic modulus is affected by individual nanofibre properties: length, diameter and bonded area (Mao et al., 2017), these properties mostly determine network density.

Lignin-preserving Fenton pre-treatment can maintain the inherent durability of softwood in terms of UV light absorptivity, antioxidativity and hydrophobicity in LMFC and self-standing films made from it. This method also results in a far better strength-stiffness combination in comparison to the case where lignin is mixed with cellulose nanofibres (Beluns et al., 2021b). Furthermore, LMFC via Fenton pre-treatment also has superior tensile stiffness and better or equal tensile strength compared to LCNF ground from semi-delignified Scots pine pulp (yield between 58 % and 84 %) (Hanhikoski et al., 2020). This is achieved with 20 % lower grinding energy and the resulting LMFC suspension has a viscosity of over a magnitude lower, thus indicating its better processability, e.g. in terms of faster dewatering and higher operation consistencies.

3.3. Costs

Pre-treatment of pine sawdust with Fenton's reagent is relatively inexpensive (Table 4). Chemical costs are almost completely due to the use of peroxide. Its price was estimated to be € 850/t (Wenderich et al., 2020) and the total cost about € 19/t at a dose of 22 kg/t. Compared to alkaline sulphonation with 55 kg/t of sodium sulphite (Ämmälä et al., 2019), at a price of € 615/t (Cavka et al., 2015), pre-treatment based on Fenton's reagent is almost 40 % cheaper.

In the production of LMFC from sawdust, the raw material is affordable, costing around € 80/t, and the expenses mostly originate from the mechanical energy applied in microfibrillation. The energy cost depends on the degree of microfibrillation; for a tensile strength level of 100 MPa (corresponding to an LS median particle size of 14 μm) the electricity cost for sawdust pre-treated with Fenton's reagent is

approximately € 750/t at an electricity price of € 70/MWh (Statista, 2020). For LMFC having an equal grade based on sulphonated sawdust (Ämmälä et al., 2019), the electricity cost would be € 830/t. Thus, the manufacturing costs of LMFC, excluding heating and pH adjustments (which are about equal in both cases), are roughly € 850/t for Fenton pre-treated and € 950/t for sulphonated sawdust, assuming 95 % yield for both LMFCs. Without any pre-treatment, by extrapolation for the same particle size (14 μm), the costs would be € 1130/t but the LMFC grade would be inferior in terms of bonding potential. The calculated costs in each case are less than the € 1300/t reported by Serra-Parareda et al. (2021), which did not include the raw material cost of bleached TMP of around € 250–300/t.

Therefore, the energy cost accounts for approximately 90 % of all manufacturing costs, and it is clear that measures to reduce grinding energy are of the utmost importance to facilitate industrial production of LMFC. The degree of microfibrillation also has an essential role and it depends on the specification of a given application. For instance, if the raw material is low-cost (like sawdust), a lower microfibrillation degree could be compensated by a higher dose when LMFC is used as reinforcement agent or binder. On the other hand, in coatings and barrier films, a smooth, highly consolidated structure is needed that cannot be substituted by a thicker layer but requires a high-grade LMFC.

3.4. Environmental aspects

LMFC production from an industrial side stream (sawdust) is sustainable, resource-efficient and eco-friendly. Fenton chemistry is environmentally sound: it does not cause emissions to air or give rise to toxic chemicals in wastewater. In addition, the dissolved organic components would remain at a low level because the yield loss is low. The process can be carried out totally sulphur-free and the main waste stream is iron-bearing sludge. Although a high Fe(II) concentration in Fenton's reagent might be beneficial for the reaction rate and efficiency, accumulation of iron can cause sludge problems. However, the Fenton pre-treatment could potentially be performed at a higher solid content and possibly even lower doses than used in this study, which would minimize sludge generation. On the other hand, iron salts could be used for the precipitation of phosphorous components, e.g. in municipal wastewaters

Table 4

Manufacturing costs for LMFCs having a particle size of 14 μm from pine sawdust using different treatments (reference, sulphonation and Fenton reaction).

	Chem. dose, kg/t	Yield, %	Raw material cost, €/t	SEC$_{gross}$ to size of 14 μm, MWh/t	H$_2$O$_2$ cost, €/t	Na$_2$SO$_3$ cost, €/t	Grinding energy, €/t	Total, €/t
Pine Fenton	22	95	84	10.7	19	–	749	852
Pine sulphonated	55	95	84	11.9	–	34	833	951
Pine ref	0	100	80	15.0	–	–	1050	1130

(Wang et al., 2014).

Although Fenton chemistry reduces energy consumption, the main environmental impact still originates from the energy intensity of wood microfibrillation, but this is unavoidable when targeting the benefits, i.e. high material efficiency, low emissions and simple processing. It should be emphasised that the grinding set-up used was not optimal in respect of energy efficiency. Through optimization, a significant reduction in energy consumption would seem plausible.

4. Conclusions

Fenton chemistry was successfully applied as a pre-treatment for the reduction of energy used in microfibrillation, simultaneously enhancing the bonding ability of micro- and nanofibres in the production of high-yield LMFC from pine sawdust. In comparison to LMFC produced without any pre-treatment, an enhanced microfibrillation rate and a 35–50 % improvement in the mechanical properties of LMFC can be achieved with low chemical costs. The reduction in energy consumption required for an equal particle size was 30 %. The LMFC made from softwood sawdust pre-treated with Fenton's reagent is inexpensive, eco-friendly and a value-added product for use as a reinforcement agent or coating in paper and cardboard or a binder in fibreboard, for example.

The Fenton pre-treatment of pine sawdust supposedly affects the microfibrillation process in two different ways. Firstly, it weakens the ultrastructure of the wood matrix, presumably via the cleavage of bonds between lignin and hemicelluloses due to attack by hydroxyl radicals within the layer that surrounds elementary fibril aggregates. This phenomenon causes a decrease in the energy needed for a given size reduction. Secondly, it has a positive effect on the chemical state of the surfaces of LMFC nanofibres, which promotes hydrogen bonding, because hemicelluloses can take part in hydrogen bonding formation due to the degraded lignin-hemicellulose network.

CRediT authorship contribution statement

Ari Ämmälä: Conceptualization, Investigation, Writing – original draft; Juho Sirviö: Writing – review & editing; Henrikki Liimatainen: Writing – Review & Editing, Resources.

Declaration of Competing Interest

The authors declare that they have no known competing financial interests or personal relationships that could have appeared to influence the work reported in this paper.

Acknowledgements

Appendix A. Supporting information

Supplementary data associated with this article can be found in the online version at doi:10.1016/j.indcrop.2022.115196.

References

Amini, E., Hafez, I., Tajvidi, M., Bousfield, D.W., 2020. Cellulose and lignocellulose nanofibril suspensions and films: a comparison. Carbohydr. Polym. 250, 117011 https://doi.org/10.1016/j.carbpol.2020.117011.

Ämmälä, A., Laitinen, O., Sirviö, J.A., Liimatainen, H., 2019. Key role of mild sulfonation of pine sawdust in the production of lignin containing microfibrillated cellulose by ultrafine wet grinding. Ind. Crops Prod. 140, 111664 https://doi.org/10.1016/j.indcrop.2019.111664.

Ämmälä, A., Sirviö, J.A., Liimatainen, H., 2021. Energy consumption, physical properties and reinforcing ability of microfibrillated cellulose with high lignin content made from non-delignified spruce and pine sawdust. Ind. Crops Prod. 170, 113738 https://doi.org/10.1016/j.indcrop.2021.113738.

Arantes, V., Milagres, A.M.F., Filley, T.R., Goodell, B., 2011. Lignocellulosic polysaccharides and lignin degradation by wood decay fungi: the relevance of nonenzymatic Fenton-based reactions. J. Ind. Microbiol. Biotechnol. 38, 541–555. https://doi.org/10.1007/s10295-010-0798-2.

Beluns, S., Gaidukovs, S., Platnieks, O., Gaidukova, G., Mierina, I., Grase, L., Starkova, O., Brazdausks, P., Thakur, V.K., 2021a. From wood and hemp biomass wastes to sustainable nanocellulose foams. Ind. Crops Prod. 170, 113780 https://doi.org/10.1016/j.indcrop.2021.113780.

Beluns, S., Platnieks, O., Gaidukovs, S., Starkova, O., Sabalina, A., Grase, L., Thakur, V. K., Gaidukova, G., 2021b. Lignin and xylan as interface engineering additives for improved environmental durability of sustainable cellulose nanopapers. IJMS 22, 12939. https://doi.org/10.3390/ijms222312939.

Bian, H., Chen, L., Dai, H., Zhu, J.Y., 2017. Integrated production of lignin containing cellulose nanocrystals (LCNC) and nanofibrils (LCNF) using an easily recyclable di-carboxylic acid. Carbohydr. Polym. 167, 167–176. https://doi.org/10.1016/j.carbpol.2017.03.050.

Brandhuber, P., Korshin, G.V., 2009. Methods for the detection of residual concentrations of hydrogen peroxide in advanced oxidation processes. WateReuse Foundation, Alexandria, VA.

Cavka, A., Martín, C., Alriksson, B., Mörtsell, M., Jönsson, L.J., 2015. Techno-economic evaluation of conditioning with sodium sulfite for bioethanol production from softwood. Bioresour. Technol. 196, 129–135. https://doi.org/10.1016/j.biortech.2015.07.051.

Diop, C.I.K., Tajvidi, M., Bilodeau, M.A., Bousfield, D.W., Hunt, J.F., 2017. Isolation of lignocellulose nanofibrils (LCNF) and application as adhesive replacement in wood composites: example of fiberboard. Cellulose 24, 3037–3050. https://doi.org/10.1007/s10570-017-1320-z.

Duan, L., Liu, R., Li, Q., 2020. A more efficient Fenton oxidation method with high shear mixing for the preparation of cellulose nanofibers. Starch - Stärke 72, 1900259. https://doi.org/10.1002/star.201900259.

FAO, 2020. Forestry production and trade 2020 (Web database). http://www.fao.org/faostat/en/#data/FO, Accessed 20th Nov 2021.

Hanhikoski, S., Solala, I., Lahtinen, P., Niemelä, K., Vuorinen, T., 2020. Fibrillation and characterization of lignin-containing neutral sulphite (NS) pulps rich in hemicelluloses and anionic charge. Cellulos 27, 7203–7214. https://doi.org/10.1007/s10570-020-03237-z.

Hellström, P., Heijnesson-Hultén, A., Paulsson, M., Håkansson, H., Germgård, U., 2014. The effect of Fenton chemistry on the properties of microfibrillated cellulose. Cellulose 21, 1489–1503. https://doi.org/10.1007/s10570-014-0243-1.

Herrera, M., Thitiwutthisakul, K., Yang, X., Rujitanaroj, P., Rojas, R., Berglund, L., 2018. Preparation and evaluation of high-lignin content cellulose nanofibrils from eucalyptus pulp. Cellulose 25, 3121–3133. https://doi.org/10.1007/s10570-018-1764-9.

Iwamoto, S., Endo, T., 2015. 3 nm Thick Lignocellulose Nanofibers obtained from esterified wood with maleic anhydride. ACS Macro Lett. 4, 80–83. https://doi.org/10.1021/mz500787p.

Iwamoto, S., Saito, Y., Yagishita, T., Kumagai, A., Endo, T., 2019. Role of moisture in esterification of wood and stability study of ultrathin lignocellulose nanofibers. Cellulose 26, 4721–4729. https://doi.org/10.1007/s10570-019-02408-x.

Jeong, S.-Y., Lee, E.-J., Ban, S.-E., Lee, J.-W., 2021. Structural characterization of the lignin-carbohydrate complex in biomass pretreated with Fenton oxidation and hydrothermal treatment and consequences on enzymatic hydrolysis efficiency. Carbohydr. Polym. 270, 118375 https://doi.org/10.1016/j.carbpol.2021.118375.

Kilpelainen, A., Peltola, H., Ryyppo, A., Sauvala, K., Laitinen, K., Kellomaki, S., 2003. Wood properties of Scots pines (Pinus sylvestris) grown at elevated temperature and carbon dioxide concentration. Tree Physiol. 23, 889–897. https://doi.org/10.1093/treephys/23.13.889.

Kishani, S., Vilaplana, F., Xu, W., Xu, C., Wågberg, L., 2018. Solubility of softwood hemicelluloses. Biomacromolecules 19, 1245–1255. https://doi.org/10.1021/acs.biomac.8b00088.

Lahtinen, P., Liukkonen, S., Pere, J., Sneck, A., Kangas, H., 2014. A comparative study of fibrillated fibers from different mechanical and chemical pulps. BioResources 9, 2115–2127.

Li, P., Sirviö, J.A., Hong, S., Ämmälä, A., Liimatainen, H., 2019. Preparation of flame-retardant lignin-containing wood nanofibers using a high-consistency mechano-chemical pretreatment. Chem. Eng. J. 375, 122050 https://doi.org/10.1016/j.cej.2019.122050.

Li, Q., Wang, A., Long, K., He, Z., Cha, R., 2019. Modified Fenton oxidation of cellulose fibers for cellulose nanofibrils preparation. ACS Sustain. Chem. Eng. 7, 1129–1136. https://doi.org/10.1021/acssuschemeng.8b04786.

Liao, J.J., Latif, N.H.A., Trache, D., Brosse, N., Hussin, M.H., 2020. Current advancement on the isolation, characterization and application of lignin. Int. J. Biol. Macromol. 162, 985–1024. https://doi.org/10.1016/j.ijbiomac.2020.06.168.

Liu, G., Huang, H., Xie, R., Feng, Q., Fang, R., Shu, Y., Zhan, Y., Ye, X., Zhong, C., 2017. Enhanced degradation of gaseous benzene by a Fenton reaction. RSC Adv. 7, 71–76. https://doi.org/10.1039/C6RA26016K.

Mao, R., Meng, N., Tu, W., Peijs, T., 2017. Toughening mechanisms in cellulose nanopaper: the contribution of amorphous regions. Cellulose 24, 4627–4639. https://doi.org/10.1007/s10570-017-1453-0.

Michalska, K., Miazek, K., Krzystek, L., Ledakowicz, S., 2012. Influence of pretreatment with Fenton's reagent on biogas production and methane yield from lignocellulosic biomass. Bioresour. Technol. 119, 72–78. https://doi.org/10.1016/j.biortech.2012.05.105.

Naimi, L.J., Collard, F., Bi, X., Lim, C.J., Sokhansanj, S., 2016. Development of size reduction equations for calculating power input for grinding pine wood chips using

hammer mill. Biomass. Convers. Biorefinery 6, 397–405. https://doi.org/10.1007/s13399-015-0195-1.

Neyens, E., Baeyens, J., 2003. A review of classic Fenton's peroxidation as an advanced oxidation technique. J. Hazard. Mater. 98, 33–50. https://doi.org/10.1016/S0304-3894(02)00282-0.

Niskanen, K.J., 1993. Strength and fracture of paper, in: Trans. of the Xth Fund. Res. Symp. Presented at the Products of Papermaking, FRC, Manchester, 2018, Oxford, pp. 641–725. https://doi.org/10.15376/frc.1993.2.641.

Normark, M., Winestrand, S., Lestander, T.A., Jönsson, L.J., 2014. Analysis, pretreatment and enzymatic saccharification of different fractions of Scots pine. BMC Biotechnol. 14, 20. https://doi.org/10.1186/1472-6750-14-20.

Oliaei, E., Berthold, F., Berglund, L.A., Lindström, T., 2021. Eco-Friendly high-strength composites based on hot-pressed lignocellulose microfibrils or fibers. ACS Sustain. Chem. Eng. 9, 1899–1910. https://doi.org/10.1021/acssuschemeng.0c08498.

Osong, S., Norgren, S., Engstram, P., 2013. An approach to produce nano-ligno-cellulose from mechanical pulp fine materials. Nord. Pulp Pap. Res. J. 28, 472–479. https://doi.org/10.3183/NPPRJ-2013-28-04-p472-479.

Packalen, T., Kärkkäinen, L., Toppinen, A., 2017. The future operating environment of the Finnish sawmill industry in an era of climate change mitigation policies. For. Policy Econ. 82, 30–40.

Rojo, E., Peresin, M.S., Sampson, W.W., Hoeger, I.C., Vartiainen, J., Laine, J., Rojas, O.J., 2015. Comprehensive elucidation of the effect of residual lignin on the physical, barrier, mechanical and surface properties of nanocellulose films. Green. Chem. 17, 1853–1866. https://doi.org/10.1039/C4GC02398F.

Rööst, C., Jönsson, T., 2001. Total organic carbon, TOC, as a tool to estimate pulp yield in the bleach plant. Nord. Pulp Pap. Res. J. 16, 261–265. https://doi.org/10.3183/npprj-2001-16-04-p261-265.

Serra-Parareda, F., Aguado, R., Tarrés, Q., Mutjé, P., Delgado-Aguilar, M., 2021. Chemical-free production of lignocellulosic micro- and nanofibers from high-yield pulps: Synergies, performance, and feasibility. J. Clean. Prod. 313, 127914 https://doi.org/10.1016/j.jclepro.2021.127914.

Sirviö, J.A., Visanko, M., 2017. Anionic wood nanofibers produced from unbleached mechanical pulp by highly efficient chemical modification. J. Mater. Chem. A 5, 21828–21835. https://doi.org/10.1039/C7TA05668K.

Sirviö, J.A., Visanko, M., 2020. Lignin-rich sulfated wood nanofibers as high-performing adsorbents for the removal of lead and copper from water. J. Hazard. Mater. 383, 121174 https://doi.org/10.1016/j.jhazmat.2019.121174.

Sirviö, J.A., Ismail, M.Y., Zhang, K., Tejesvi, M.V., Ämmälä, A., 2020. Transparent lignin-containing wood nanofiber films with UV-blocking, oxygen barrier, and anti-microbial properties. J. Mater. Chem. A 8, 7935–7946. https://doi.org/10.1039/C9TA13182E.

Sirviö, J.A., Isokoski, E., Kantola, A.M., Komulainen, S., Ämmälä, A., 2021. Mechanochemical and thermal succinylation of softwood sawdust in presence of deep eutectic solvent to produce lignin-containing wood nanofibers. Cellulose. https://doi.org/10.1007/s10570-021-03973-w.

Spence, K.L., Venditti, R.A., Rojas, O.J., Habibi, Y., Pawlak, J.J., 2011. A comparative study of energy consumption and physical properties of microfibrillated cellulose produced by different processing methods. Cellulose 18, 1097–1111. https://doi.org/10.1007/s10570-011-9533-z.

Statista, 2020. Prices of electricity for industry in Finland from 1995 to 2020 (Web database). https://www.statista.com/statistics/595853/electricity-industry-price-finland, Accessed 20th Nov 2021.

Switzer, L.H., Klingenberg, D.J., 2004. Flocculation in simulations of sheared fiber suspensions. Int. J. Multiph. Flow. 30, 67–87. https://doi.org/10.1016/j.ijmultiphaseflow.2003.10.005.

Tufail, A., Price, W.E., Hai, F.I., 2020. A critical review on advanced oxidation processes for the removal of trace organic contaminants: A voyage from individual to integrated processes. Chemosphere 260, 127460. https://doi.org/10.1016/j.chemosphere.21020.127460.

The sawmill industry - Handbook E-Book. In: Varis, R. (Ed.), 2018. Suomen Sahateollisuusmiesten Yhdistys ry.

Vasquez-Medrano, R., Prato-Garcia, D., Vedrenne, M., 2018. Chapter 4 - Ferrioxalate-mediated processes, in: Ameta, S.C., Ameta, R. (Eds.), Advanced oxidation processes for waste water treatment. Academic Press, pp. 89–113. https://doi.org/10.1016/B978-0-12-810499-6.00004-8.

Visanko, M., Sirviö, J.A., Piltonen, P., Sliz, R., Liimatainen, H., Illikainen, M., 2017. Mechanical fabrication of high-strength and redispersible wood nanofibers from unbleached groundwood pulp. Cellulose 24, 4173–4187. https://doi.org/10.1007/s10570-017-1406-7.

Walter, K., 2013. The use of Fenton chemistry for reducing the refining energy during TMP production the effect of free ferrous and free or chelated ferric ions. FSCN, Sundsvall; Mid Sweden University.

Walter, K., Paulsson, M., Wackerberg, E., 2009. Energy efficient refining of black spruce TMP by using acid hydrogen peroxide: Part 1. A pilot plant study. Nord. Pulp Pap. Res. J. 24, 255–265. https://doi.org/10.3183/npprj-2009-24-03-p255-265.

Wang, Y., Tng, K.H., Wu, H., Leslie, G., Waite, T.D., 2014. Removal of phosphorus from wastewaters using ferrous salts – a pilot scale membrane bioreactor study. Water Res. 57, 140–150. https://doi.org/10.1016/j.watres.2014.03.029.

Wen, Y., Yuan, Z., Liu, X., Qu, J., Yang, S., Wang, A., Wang, C., Wei, B., Xu, J., Ni, Y., 2019. Preparation and characterization of lignin-containing cellulose nanofibril from poplar high-yield pulp via TEMPO-mediated oxidation and homogenization. ACS Sustain. Chem. Eng. 7, 6131–6139. https://doi.org/10.1021/acssuschemeng.8b06355.

Wenderich, K., Kwak, W., Grimm, A., Kramer, G.J., Mul, G., Mei, B., 2020. Industrial feasibility of anodic hydrogen peroxide production through photoelectrochemical water splitting: a techno-economic analysis. Sustain. Energy Fuels 4, 3143–3156. https://doi.org/10.1039/D0SE00524J.

Wu, C., Chen, W., Gu, Z., Li, Q., 2021. A review of the characteristics of Fenton and ozonation systems in landfill leachate treatment. Sci. Total Environ. 762, 143131 https://doi.org/10.1016/j.scitotenv.2020.143131.

Xie, Y., Xiao, Z., Mai, C., 2015. Degradation of chemically modified Scots pine (Pinus sylvestris L.) with Fenton reagent. Holzforschung 69, 153–161. https://doi.org/10.1515/hf-2014-0067.

Xu, E., Wang, D., Lin, L., 2020. Chemical structure and mechanical properties of wood cell walls treated with acid and alkali solution. Forests 11, 87. https://doi.org/10.3390/f11010087.

Yousefi, H., Azari, V., Khazaeian, A., 2018. Direct mechanical production of wood nanofibers from raw wood microparticles with no chemical treatment. Ind. Crops Prod. 115, 26–31. https://doi.org/10.1016/j.indcrop.2018.02.020.

Yu, H.-T., Chen, B.-Y., Li, B.-Y., Tseng, M.-C., Han, C.-C., Shyu, S.-G., 2018. Efficient pretreatment of lignocellulosic biomass with high recovery of solid lignin and fermentable sugars using Fenton reaction in a mixed solvent. Biotechnol. Biofuels 11, 287. https://doi.org/10.1186/s13068-018-1288-4.

Yuan, T., Zeng, J., Wang, B., Cheng, Z., Chen, K., 2021. Lignin containing cellulose nanofibers (LCNFs): lignin content-morphology-rheology relationships. Carbohydr. Polym. 254, 117441 https://doi.org/10.1016/j.carbpol.2020.117441.

Zhao, Y., Shakeel, U., Saif Ur Rehman, M., Li, H., Xu, X., Xu, J., 2020. Lignin-carbohydrate complexes (LCCs) and its role in biorefinery. J. Clean. Prod. 253, 120076 https://doi.org/10.1016/j.jclepro.2020.120076.

Zhu, Y., Plaza, N., Kojima, Y., Yoshida, M., Zhang, J., Jellison, J., Pingali, S.V., O'Neill, H., Goodell, B., 2020. Nanostructural analysis of enzymatic and non-enzymatic brown rot fungal deconstruction of the lignocellulose cell wall. Front. Microbiol. 11, 1389. https://doi.org/10.3389/fmicb.2020.01389.